

Magnetic polarons in weakly doped high- T_c superconductors.

E.M. Hankiewicz, R. Buczko, and Z. Wilamowski

*Institute of Physics, Polish Academy of Sciences,
al. Lotników 32/46, PL 02-668 Warsaw Poland*

We consider a spin Hamiltonian describing d - d exchange interactions between localized spins d of a finite antiferromagnet as well as p - d interactions between a conducting hole (p) and localized spins. The Hamiltonian is solved numerically with use of Lanczos method of diagonalization. We conclude that p - d exchange interaction leads to localization of magnetic polarons. Quantum fluctuations of the antiferromagnet strengthen this effect and make the formation of polarons localized in one site possible even for weak p - d coupling. Total energy calculations, including the kinetic energy do not change essentially the phase diagram of magnetic polarons formation. We find that for parameters reasonable for high- T_c superconductors (i.e. the effective mass about few electron masses and the ratio of p - d to d - d exchange integral between ten and thirty) a polaron localized in one lattice cell as well as a small feron can form. For reasonable values of the dielectric function and p - d coupling constant the contributions of magnetic and phonon terms in the formation of a polaron in weakly doped high- T_c materials are comparable.

PACS numbers: 74.72.-h, 74.20.-z, 71.38.-k

I. INTRODUCTION

The role of electron phonon and spin exchange in the formation of polarons, bi-polarons and stripes in CuO_2 based high- T_c materials is a matter of extensive discussion from the very moment high- T_c superconductors were discovered.

On the one hand experimental observations of the isotope effect indicate the role of phonon interactions in the formation of the superconducting state. On the other hand, angularly resolved photoemission¹, transport² and tunneling microscopy measurements³ show d -symmetry of the order parameter indicates the main role played by magnetic interactions. Although some authors underline the role of both effects⁴, the solution of full Hamiltonian including magnetic and phonon interactions is complicated and usually these contributions are calculated separately.

The concept of the phonon polaron was introduced by Pekar⁵ and Fröhlich^{6,7} many years ago and was adapted to high- T_c superconductors by Alexandrov and Mott⁸. The energy of phonon coupling for high- T_c is estimated by Alexandrov and Mott to be of the order of a fraction of electronvolt. In another work Alexandrov⁹ proposed that the narrowing of d -electron band by the polaron effect and the formation of phonon bipolarons increases the critical temperature to about 100 K.

However, because of the dominant contribution of d -symmetry to the order parameter of high- T_c superconductors, magnetic interactions are the most often considered recently. The modeling of such interactions is difficult because it is necessary to include the role of conducting (p) holes as well as localized (d) electrons.

In the case of weak p - d couplings a linear response of

the antiferromagnet (AF) can be assumed and a phenomenological model of magnetic susceptibility can be used. Such a model was introduced by Millis, Monien, Pines¹⁰.

Zhang and Rice¹¹, in turn, describe the case of strong hybridization between the $3d$ states of Cu and $2p$ states of O. When the hybridization is much greater than the kinetic energy of the carriers it is possible to limit the description to the ground singlet state and the authors show that in such a case a one band model can be used. The Zhang-Rice model (called t - J) is at present the most often used to describe the cuprate superconductors (for a review see¹²). Unfortunately different techniques of approximations applied by different authors lead sometimes to contradictory solutions of t - J , as it is in the case of the stripe formation^{13,14}.

Most of models in use base upon the classical antiferromagnet approach. They often yield conclusions which are in accordance with experimental results^{15,16}. It seems, however, that in some cases^{17,18,19} antiferromagnetic quantum fluctuations may play a role and can not be omitted.

Even considering of magnetic interactions alone, neither model is universal. It makes the comparison of phonon and magnetic energies very complicated. Moreover, the lack of basic material parameters such as the bare effective mass, dielectric constant, and exchange constants increases the difficulty even further. On the one hand, any revision of the models is not possible without these parameters while on the other, the complex experimental data can not be interpreted well without a correct theory. For example, the experimentally observed effective mass is decorated by the coupling of the carrier with phonons and magnons. Without

a proper model one cannot evaluate the bare effective mass or find the part of the effective mass corresponding to phonon or magnetic interactions.

In this paper we use a model which allows us to investigate the cases of weak, strong and intermediate p - d coupling. Thus we can compare the phonon and magnetic contributions to the formation of a polaron in weakly doped high- T_c superconductors for a wide range of parameters. We calculate the magnetic exchange interactions strictly, while the phonon contribution is evaluated in the framework of the Fröhlich theory^{6,7,8}.

In section 2, we describe the Hamiltonian and the method of finding the ground and excited states of the system. In section 3 we analyze the exchange spin interactions only. In section 4 we construct and analyze phase diagram for the formation of different magnetic polarons. In section 5 we compare the energies of phonon and magnetic polarons. At the end we summarize our paper in section 6.

II. THEORY

We study a system which consists of spins localized on the d -shells and mobile p -like holes. The localized spins are treated in the quantum antiferromagnet model, i.e., none of the Neel sublattices are chosen a priori. We consider finite one- and two- dimensional clusters as well as the infinite system. The latter is simulated by using periodic boundary conditions (PBC) and an extrapolation to an infinite size. The spin interactions in the system and the kinetic energy of the p hole is described by the Hamiltonian:

$$H = 2J_{dd} \sum_{\langle i,j \rangle} S_i S_j + \frac{1}{2} J_{pd} \sum_{i,\alpha,\beta} S_i c_{i\alpha}^+ \sigma_{\alpha\beta} c_{i\beta} + t_{ij} \sum_{i,j,\alpha} c_{i\alpha}^+ c_{j\alpha} \quad (1)$$

where S_i is the effective spin of the nine core d -electrons ($3d^9$), the summation was taken under the pairs of neighboring spins $\langle i,j \rangle$, $\sigma_{\alpha\beta}$ are the Pauli matrices of the carrier spin s , J_{pd} is the Kondo parameter divided by the volume of elementary cell, J_{dd} is the exchange integral between d - d spins, t_{ij} is the hopping matrix element to the neighbor, $c_{i\alpha}^+$, $c_{i\alpha}$ are the operators of creation and annihilation of a hole on the i -th site, with the projection of spin $1/2$ on the quantization axis equal α respectively. Such a Hamiltonian is known in the literature as the spin-fermion model. It was successfully used in description of high- T_c superconductors^{15,20,21,22}. However, usually the spins were treated classically. Here we present the approach

which allows for consideration all the spins in a quantum treatment. It broadens the possible range of solutions of spin-fermion model (for possible magnetic phases when localized spins are treated classically see for example²³).

We look for the eigenstates of the Hamiltonian (1) in the form of the product of the orbital wave vector, Ψ , and of the spin state vector of local and carrier spins X_S :

$$\Psi \cdot X_S \quad (2)$$

In the space of the single hole occupation at site $i = 1, \dots, N$

$$\Psi = \sum_i \varphi(i) u_i \quad (3)$$

where $u_i = |0, 0, \dots, 1, 0, 0 \dots\rangle$ is the occupation vector of the hole at i -th site and $\varphi(i)$ is the corresponding probability amplitude.

We use the variational method of solving the eigenproblem. We treat Ψ as the trial function which is normalized by the condition

$$\sum_i |\varphi(i)|^2 = 1 \quad (4)$$

For the eigenstates of the form done by Eq. (2) with fixed Ψ the diagonalization of the kinetic and exchange terms of Hamiltonian (1) can be done separately.

$$H' = \langle \Psi | H | \Psi \rangle = T + H_s \quad (5)$$

The kinetic energy, T , does not depend on the spin state X_S and can be easily evaluated from the probability amplitude of the carrier, $\varphi(i)$

$$T = z |t_1| - 2 |t_1| \sum_{\langle i,j \rangle} \varphi(i) \varphi(j) \quad (6)$$

if only the hopping to the nearest neighbors, t_1 is considered, and z is the number of the nearest neighbors. The term $z|t_1|$ has been added to have zero kinetic energy for fully delocalized states.

The evaluation of the exchange energy needs diagonalization of the spin Hamiltonian:

$$H_s = 2J_{dd} \sum_{\langle i,j \rangle} S_i S_j + \sum_i j_{pd}(i) S_i s \quad (7)$$

Here s is the spin operator of the carrier spin and the p - d exchange integrals are given by

$$j_{pd}(i) = J_{pd} |\varphi(i)|^2 \quad (8)$$

We use Lanczos method of diagonalization of the spin Hamiltonian (7). Diagonalization of matrices for AF cluster with $N \leq 20$ is possible with the PC computer. For larger clusters the calculation time rapidly increases.

A detailed study of quantum coupling between spins within the polaron in an antiferromagnetic medium is the main goal of this paper. We focus our analysis on the gain E_{ex} of the spin exchange energy and the correlation functions.

E_{ex} is the difference between the energy of the ground state of the unperturbed antiferromagnet E_{dd}^0 (when $J_{pd} = 0$), and the exchange energy of the whole system when the carrier is coupled to the antiferromagnet $E_{dd} + E_{pd}$ i.e.:

$$E_{ex} = E_{dd}^0 - (E_{dd} + E_{pd}) \quad (9)$$

In this way we analyze the zero temperature case only.

We found that for a weak p - d coupling the gain of the exchange energy, E_{ex} , is half of the p - d coupling energy,

$$E_{ex} = -E_{pd}/2 \quad (10)$$

The Hamiltonian includes neither effects of external magnetic field nor any other terms which could lead to the symmetry breaking and to the formation of Neel sublattices. As a consequence, the mean values of the magnetic moments of each spin of this system are exactly equal zero. Because of this we describe the spin structure of the antiferromagnetic polarons (AFP) and the mechanism of the magnetic polaron formation by means of correlators between spins of AF $\langle S_i S_j \rangle$ and between the AF spin and that of an additional hole $\langle s S_i \rangle$.

$$\langle s S_i \rangle = \langle X_S | s S_i | X_S \rangle \quad (11)$$

Hamiltonian (1) does not contain any phonon term. In general, the coupling of the carrier to the lattice polarization and the exchange interactions act together to form the polaron. Both compete with the kinetic energy. The minimum of the total energy determines the polaron structure. In this paper, however, neglecting phonon term we discuss the minimization of the sum of exchange and kinetic energies. We are only interested in the gain of the exchange energy, E_{ex} , and we look for the minimum of the sum of the exchange and kinetic energies. In other words, we investigate the possibility of

the formation of a pure magnetic polaron. Afterwards, we compare the exchange and the phonon contributions to the energy of the polaron formation.

The phonon term is treated within the simplest possible approach. It is calculated from Fröhlich interaction with optical phonons. It is known⁸ that in the range of parameters typical for high- T_c superconductors small phonon polarons are formed. Their energy is given by:

$$E_{ph} \approx \frac{q_D e^2}{\pi \kappa} \quad (12)$$

where $q_D = \left(\frac{6\pi^2}{V}\right)^{1/3}$ is the Debye momentum, $\frac{1}{\kappa} = \frac{1}{\varepsilon} - \frac{1}{\varepsilon_0}$; $\varepsilon, \varepsilon_0$ are dynamic and static dielectric constants respectively, and e is the electron charge.

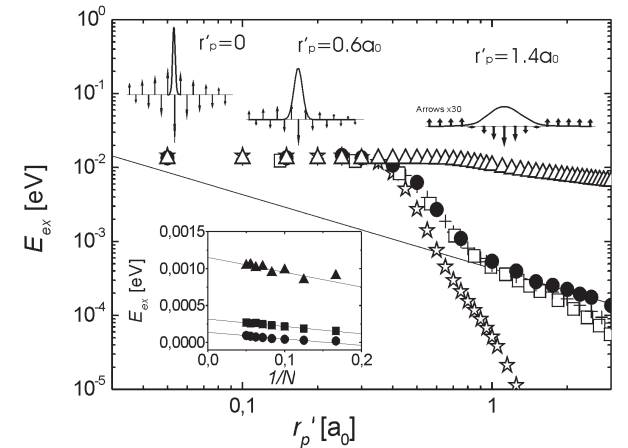


FIG. 1: The exchange energy gain, E_{ex} , obtained for a Gauss trial function (see Eq. 13) is presented as a function of polaron radius r'_p , for 1D open chain (crosses), for 1D chain with periodic boundary conditions (PBC) (open squares) and for a 4×4 square with PBC (open stars). Open triangles show the dependence $E_{ex}(r'_p)$ for a comb-like carrier trial function (see Eq. 23) and 1D AF chain of 16 spins. In the inset the extrapolation of E_{ex} to infinite AF 1D cluster is shown by filled triangles, squares and circles for $r'_p = 0.75a_0$, $r'_p = 1.5a_0$ and $r'_p = 3a_0$ respectively. In the icons arrows show the correlators between the carrier spin, s , and d spins of AF for a small AFP ($r'_p = 0$), medium AFP ($r'_p = 0.6a_0$) and large AFP ($r'_p = 1.4a_0$). For a large AFP, the arrow size is multiplied 30 times for clarity. Solid curves show trial functions.

III. SPIN STRUCTURE OF MAGNETIC POLARONS

We examine various types of trial functions φ . Depending on the size and shape of the carrier distribu-

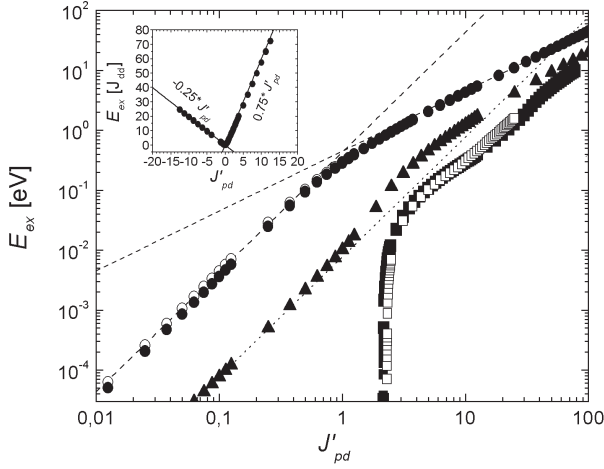


FIG. 2: The exchange energy gain, E_{ex} , from formation of different magnetic polarons as a function of J'_{pd} . The data for a small AFP were obtained for a 1D chain with PBC (open circles) and for a 2D 4×4 square with PBC (filled circles). The data obtained for a trial function homogeneously distributed on all AF spins are shown by open and filled squares for a 1D chain with PBC and 2D 4×4 with PBC respectively. Results for a trial function distributed on two neighbor AF spins and a 1D chain with PBC are drawn by filled triangles. The dashed lines show the range of quadratic and linear dependencies of E_{ex} versus J'_{pd} . The dotted line emphasizes the more than quadratic dependence of $E_{ex}(J'_{pd})$. The inset shows the gain of the exchange energy, E_{ex} , as a function of J'_{pd} for a small AFP.

tion, $|\varphi|^2$, as well as on the value of exchange constants various types of magnetic polarons, characterized by very different spin structures, can be found. The analysis of the dependence of the energy gain due to polaron formation, as well as correlators functions, on the polaron size (Fig. 1) and the p - d exchange (Fig. 2) allows us to distinguish five types of AFP.

A. Large AFP The size, r'_p , of such a polaron is much greater than the lattice constant a_0 and the anti-ferromagnetic correlation range. Thus, for its description the theory of the linear response can be applied. For very large polarons the local magnetization becomes proportional to the local carrier density¹⁰.

B. Medium AFP The size of such a polaron is comparable or smaller than the correlation range, ξ , but bigger than $0.5a_0$ (see Fig. 1). The induced polarization is of staggered character and the carrier interacts with few local spins of different orientation.

C. Small AFP A small polaron is localized within a

single elementary cell. In the limit of very strong p - d coupling the small AFP corresponds to the Zhang-Rice polaron. Here, the carrier spin becomes fully compensated by the local spin.

D. Ferron It forms when the p - d exchange is strong enough to break AF bonds and to induce a local magnetic moment²⁴.

E. Comb like AFP Such a polaron corresponds to the case when the carrier is distributed on a single Neel sublattice only. The staggered polarization is the dominant response of the AF medium^{21,25}.

The clear difference between AFP of different sizes is seen in Fig. 1, where the energy gain, E_{ex} , is plotted as a function of the polaron size r'_p . Gaussian trial function

$$|\varphi(i)|^2 = A \exp \left[-\frac{(r_i - r_0)^2}{2r_p'^2} \right] \quad (13)$$

where A is a normalization factor and $r_i - r_0$ is the distance from central spin, was used to calculate almost all curves. The curve plotted by triangles, however, was calculated using another trial function and is responsible for the formation of a comb-like AFP. Comb-like polarons will be discussed in part III E.

The calculations were performed for weak p - d coupling for 1D and 2D AF clusters. The number of AF bonds has been assumed to be twice as big for 2D as for a 1D cluster, where the number of ligands is two times smaller. To compare the results for one and two dimensional AF cluster we introduce the following quantity, $J'_pd = J_{pd}/(2zJ_{dd})$, which describes the ratio of p - d to d - d coupling normalized by the number of AF bonds, $2z$. Ratio of the p - d to the d - d exchange energies defined this way is the same for 1D and 2D AF clusters. Moreover, $J'_{pd} < 1$ describes the range of weak p - d coupling, while $J'_{pd} > 1$ that of strong p - d coupling, independent of the dimension of the AF cluster. J'_{pd} is set 1/4 in Fig. 1. Here the small AFP corresponds to $r'_p < 0.4a_0$, medium to $0.4a_0 < r'_p < a_0$, and large to $r'_p > a_0$. The crosses correspond to a 1D chain of 16 spins with $S = 1/2$ and the open squares to the same chain with periodic boundary conditions (PBC). The stars correspond to a two dimensional $4 \times 4 = 16$ spin cluster also with PBC. The center of the polaron, r_0 , is chosen at one of the central spins.

The dependence of the exchange energy gain on the chain length is shown in the inset. The linear dependence of the E_{ex} on the inverse chain size $1/N$ makes the extrapolation to an infinite chain possible. The extrapolated values of the energy gain are shown by full circles in Fig. 1.

The results of numerical calculations performed for small and medium AFP in 1D case are reasonable even without extrapolation to infinite clusters. Because of that we assume that also for the 2D case the energy of small and medium polarons can be found with reasonable accuracy. Unfortunately, because our computational method is limited to small size clusters, we can not carry out full extrapolation analysis for large AFP in 2D clusters.

Comparison of numerical results for open chains and chains with PBC shows that the use of PBC does not lead to an improvement of the convergence of numerical results with the cluster size. In part, this is an effect of the normalization condition given by (Eq. 4) and of specific properties of the dangling spins at the cluster border.

A. Large AFP

The numerical results, with the characteristic dependence of the exchange energy gain decreasing as $1/r_p'$ for 1D AF, can be approximated by an analytical solution in which the magnetic susceptibility of AF is described by two phenomenological parameters. The analytical solution gives a better description of large AFP while the comparison with the numerical results allows to explain the physical meaning of the phenomenological parameters.

For simplicity in the analytical approximation we use an exponential distribution of carrier density:

$$|\varphi(r')|^2 = \frac{1}{2r_p} \exp\left(-\frac{|r' - r_0|}{r_p}\right) \quad (14)$$

where r_0 is the center of the density distribution and r_p is connected with the polaron size r_p' in the following way: $r_p'^2 = r_p^2/2$. We assume that the susceptibility in wave vector space can be described by the phenomenological formula introduced in the Millis, Monien, and Pines model¹⁰.

$$\chi(q) = \chi_{q_0} \frac{1}{1 + (q - q_0)^2 \xi^2} \quad (15)$$

In the last formula q is the wave vector, $q_0 = \pi/a_0$ corresponds to the staggered magnetization. The parameters χ_{q_0} and ξ are phenomenological parameters describing the staggered magnetic susceptibility and the spin correlation length, respectively.

The effective field, caused by the p - d coupling (second term in Hamiltonian 7) acting on the local spin takes for the carrier distribution, described by Eq. 14 the form:

$$H_{eff}(r') = \frac{J_{pd}a_0}{4g\mu_B r_p} \exp\left(-\frac{|r' - r_0|}{r_p}\right) \quad (16)$$

Within the model of continuous media an effective field acting at a point r' results in magnetization at the point r

$$M(r) = \int dr' \chi(r - r') H_{eff}(r') \quad (17)$$

Such an approach takes into account the non-local effects of correlated systems, but neglects the atomic structure of AF. Because of that it can be applied only for $r_p, \xi \gg a_0$. But it can be also applied in the case of $r_p < a_0$, when the center of the polaron is localized in the center of the elementary cell. This is equivalent to the case when a polaron is localized within a single elementary cell.

For large AFP, i.e. for $r_p \gg \xi$, the integral 17 takes a simple form:

$$M(r) = \frac{J_{pd}a_0\chi_{q_0}}{16\pi^2 g\mu_B \xi^2} \frac{1}{q_0^2 r_p} \exp\left(-\frac{|r' - r_0|}{r_p}\right) \quad (18)$$

According to formula 18 the magnetization induced by a large AFP is homogeneous. It is described by the same spatial dependence as the carrier density. In the icon in Fig. 1 the correlators between the carrier spin, s and the consecutive local spins, S_i , for a large AFP is presented. It also shows that for a large AFP the induced magnetization is smooth and proportional to the carrier density. In that sense the analytical solution is equivalent to the numerical one.

The gain of the exchange energy, E_{ex} , is a half of the p - d exchange energy, E_{pd} (see Eq. 10) which is described by an integral of the product of the magnetization (Eq. 18), and the effective field (Eq. 16). For a large AFP it takes a simple form:

$$E_{ex} = \frac{(J_{pd}a_0)^2 \chi_{q_0}}{256\pi^2 (g\mu_B)^2 \xi^2 q_0^2 r_p} \quad (19)$$

The absolute value of E_{ex} and its dependence on the d - d exchange and on the correlation length cannot be analyzed within the discussed phenomenological approach. An evaluation of E_{ex} can be done by numerical calculations. If one attributes the correlation length to the cluster size then the comparison of Eq. 19 with the numerical result, showing that the energy gain is almost independent of the chain length (see inset to Fig. 1), leads to the conclusion that χ_{q_0} , for a large 1D polaron,

$$\chi_{q_0} \propto \frac{\xi^2}{J_{dd}} \quad (20)$$

is proportional to the square of the correlation radius, ξ . We found out that the character of the obtained dependencies does not change if a Gauss trial function was applied.

In the 2D case, we were not able to find analytical solutions, neither for exponential nor Gaussian trial functions. However, the results of numerical integration indicate that large AFP in a 2D system are characterized by a faster decrease of the energy gain with the polaron size in comparison to the 1D case. The energy scales with $1/r_p^2$ instead of $1/r_p$ as in the 1D case.

Since a numerical diagonalization of the spin Hamiltonian is possible only in the case of small clusters, we are not able to study the dependence of χ_{q_0} on the correlation range, ξ , for a large 2D polaron.

Summarizing, the large AFP is characterized by a smooth magnetization of the antiferromagnet, proportional to the carrier density. Because for a 2D polaron the gain of the exchange and the kinetic energies scale with the inverse square of the polaron size two scenarios are possible: (i) no polaron can be formed when the kinetic energy overcomes the exchange one, or, in the opposite case, (ii) the minimum of the total energy occurs for the polaron radius tending to zero (see also Fig. 6). In that case, however, it is no longer a large polaron and a different approximation should be considered.

B. Medium AFP

As it is shown in Fig. 1, with a decrease of the polaron radius the exchange energy gain does not follow the $1/r_p'$ dependence, but for $r_p' < a_0$ a sharp increase of E_{ex} is seen. For 1D the increase of E_{ex} is by a factor of 10, as compared to the extrapolated $1/r_p'$ dependence, and for 2D the increase is even bigger. The decrease of the polaron radius is also accompanied by a change of the character of induced magnetization in the AF medium. As it is shown by icons in Fig. 1, numerical calculations predict a smooth magnetization for $r_p' \geq a_0$ but a staggered one for $r_p' < a_0$.

The same character of the staggered response of the AF is also predicted from the analytical solution. For a medium AFP, when $r_p < \xi$ and polaron is delocalized on few AF spins, the integral in Eq. 17 can be approximated by the expression:

$$M(r) \cong \frac{J_{pd}a_0\chi_{q_0}}{16\pi^2g\mu_B\xi} \frac{1}{1+q^2r_p^2} \exp\left(-\frac{|r'-r_0|}{\xi}\right) \times \cos[q_0(r-r_0)]. \quad (21)$$

Here the position of the center of polaron has been assumed to be located at a chosen spin. The staggered

response of AF is spread within the correlation length, ξ , which is assumed to be much greater than the distribution of the carrier, r_p . Because of that one can introduce two different quantities describing the polaron size. The radius of the charge distribution corresponds to r_p , while the magnetic polaron radius corresponds to ξ . This duality is the consequence of non local properties of the AF system.

Within the same approximation E_{ex} for the 1D medium AFP is described by the analytical formula:

$$E_{ex} = \frac{(J_{pd}a_0)^2\chi_{q_0}}{128\pi^2(g\mu_B)^2\xi} \left(1 + \frac{r_p}{\xi}\right) \frac{1}{(1+r_p^2q_0^2)^2} \quad (22)$$

Thus, the gain of exchange energy is predicted to be bigger as compared to the extrapolation of the large AFP. For the medium AFP, the ratio r_p/ξ is a small correction as compared to unity. When $r_p \gg a_0$ the unity in the denominator can be omitted, and E_{ex} is then expected to change with $1/r_p^4$.

The rapid increase of E_{ex} with the decrease of polaron radius means that the medium AFP has a tendency to localization. The character of the analytical solution agrees well with the numerical results, but comparison of Eq. 22 with the results of numerical diagonalization does not lead to any simple conclusion about the dependence of χ_{q_0} on the correlation range, ξ .

For weak p - d coupling the gain of the exchange energy E_{ex} increases with the square of J'_{pd} . It is seen as well in Eq. 22 as in Fig. 2, where numerical results for a medium size AFP are presented (filled triangles). For $J'_{pd} > 1$ the analytical solution is not valid. The numerical calculations show that for a bigger J'_{pd} a more complex mechanism occurs. The AF bonds become broken and a ferron-like polaron forms. The details are described in part IIID.

C. Small AFP

When the polaron radius becomes comparable to the size of the elementary cell the gain of the exchange energy, E_{ex} , saturates. The plateau in Fig. 1 corresponds to the case when the polaron is localized in a single elementary cell. Within our formalism it corresponds to the condition $r_p' < a_0$. The numerical results weakly depends on the size of the considered AF cluster and on the type of boundary conditions.

The numerical data can be well approximated by the analytical formula given in (Eq. 22). The last term of (Eq. 22) reflects the transition from small to medium polaron.

The magnetization of the antiferromagnet which is induced by the small AFP is similar to that of the

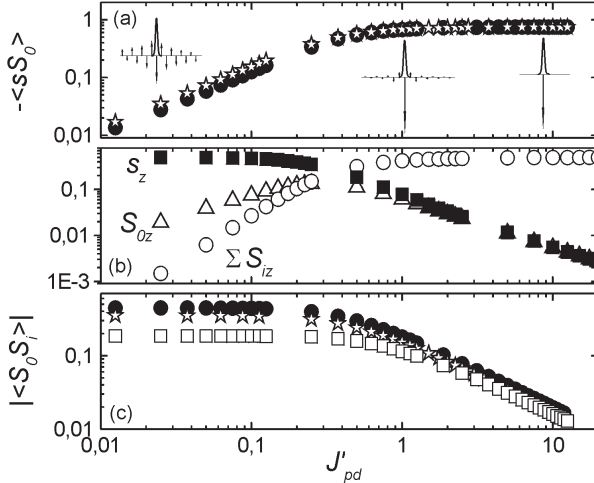


FIG. 3: (a) The correlator, $|\langle sS_0 \rangle|$, between the carrier spin, s , and d spin on which the carrier is localized S_0 , as a function of J'_{pd} for 1D chain with PBC (filled circles) and 2D 4×4 square with PBC (open stars). In the icons the correlators between the carrier spin, s and consecutive d spins of AF chain for different values of J'_{pd} shown in figure. (b) The z -component of carrier spin, s_z , of central spin S_{0z} , as well as the sum of AF spins $\sum_i S_{iz}$ are shown for an open chain of 16 spins as a function of J'_{pd} . (c) The correlator between the spin on which the polaron is acting and the nearest (filled circles) and the next nearest neighbor spin (open squares) for a chain of 16 spins. The correlator between the spin on which the polaron is acting and the nearest neighbor spin for a 2D 4×4 square with PBC is presented by stars.

medium AFP. The correlators of local spins with the spin of carrier are shown by the icons in Fig. 1. The analytical solution for magnetization in 1D is given by Eq. 21 in the limit $r_p \ll a_0 \ll \xi$.

For the 2D case the numerical integration leads to the conclusion that the gain of exchange energy scales with $1/\xi^2$.

Additionally our numerical results show that E_{ex} does not depend on the size of the cluster. Because of that we conclude that E_{ex} is independent of the correlation range ξ . Consequently, the phenomenological parameter χ_{q_0} should be considered as proportional to ξ for 1D and to ξ^2 for 2D, when applied to a small polaron (for comparison with a large AFP see Eq. 20). We return to this problem in section F.

The dependence of the numerically evaluated E_{ex} on the normalized ratio p - d to d - d exchange J'_{pd} is shown by circles in Fig. 2. There is no considerable difference between 1D and 2D cases. For weak p - d coupling E_{ex} increases with J'^2_{pd} . The upper limit of this quadratic dependence corresponds to the case when the p - d coupling is equal to the d - d exchange. For higher J'_{pd} the

energy increases linearly.

The correlator $\langle sS_0 \rangle$, between the carrier spin, s , and d spin on which the carrier is localized, S_0 , is shown in Fig. 3a. In the range of weak p - d couplings the magnetization of the local spin, as seen by the carrier spin, $\langle sS_0 \rangle$, increases linearly and saturates for the strong ones. This corresponds to quadratic and linear dependence of E_{ex} versus J'_{pd} , respectively. For strong J'_{pd} the correlator $\langle sS_0 \rangle$ is constant and equal $-3/4$ what means that the local spin S_0 is compensated by the spin of carrier, s .

The icons in Fig. 3a show the correlators between the carrier spin s and the consecutive d spins of AF chain for different values of J'_{pd} . They show that a small polaron induces a staggered magnetization within the AF correlation range, ξ . But the amplitude of the induced staggered magnetization, as seen by the carrier spin, s , varies with J'_{pd} . The increase of the correlator $\langle sS_0 \rangle$ is accompanied by a reduction of the correlators between the carrier spin and other d spins.

Also the correlator of the spin S_0 with neighboring spins S_i , $\langle S_0S_i \rangle$, decreases systematically when J'_{pd} increases. The dependence of correlator for the nearest and the next nearest neighbor are shown in Fig. 3c. The correlators are not affected by the presence of a weak polaron, but in the limit of J'_{pd} they decrease as $1/J'_{pd}$.

The ground state of a system consisting of a carrier with $s = 1/2$ and an AF cluster of an even number of local spins is a spin doublet, for the whole range of p - d coupling constants, J'_{pd} . However, depending on the value of J'_{pd} , the magnetic moment can be transferred from the carrier to the system of local spins. For a non-interacting spin s , or for a very weak p - d coupling, the carrier spin is characterized by a magnetic moment while the total magnetic moment of local spins is zero. In Fig. 3b the z -component of the carrier spin, s_z , the local spin S_{0z} and the sum of all local spins $\sum_i S_{iz}$ are plotted as a function of the strength of p - d coupling. We distinguish the z -direction by putting the small magnetic field which does not perturb the spin structure of polaron. With an increase of p - d coupling the magnetic moment is transferred from the carrier to the local spins. For a very strong p - d coupling, the magnetic moment of local spins $\sum_i S_{iz}$ saturates at value $1/2$. Simultaneously, the magnetic moments associated with the carrier spin, s_z , and of the local spin, S_{0z} , vanish. The magnetic moments of the local spins, $\sum_i S_{iz}$, are distributed in a staggered way among the whole cluster.

The small polaron in the limit of strong p - d coupling, $J'_{pd} \gg 1$ is equivalent to the Zhang-Rice (ZR) polaron. Here the spins, s and S_0 , are compensated and form a local singlet state, not coupled to other local spins, S_i (see Fig. 3c and the icon in Fig. 3a.). On the other hand,

the formation of a central pair of compensated spins is accompanied by a transfer of the magnetic moment to the neighboring local spins and formation of staggered magnetization around the central cell. Such an effect is known in the literature and described very detailed for example in²⁶. The reconstruction of AF bonds in the vicinity of the small AFP is driven by a gain of d - d exchange energy. It is of the order of J_{dd} . It is a small contribution to the whole energy of the ZR polaron but becomes important for $J'_{pd} \cong 1$. Moreover, the reconstruction of the AF environment should be taken into account when interactions between separate polarons are discussed.

Summarizing, the small AFP in the range of intermediate p - d coupling (typical for high- T_c superconductors) is not equivalent the ZR polaron. The carrier spin is also partially correlated with AF spins in the vicinity of local singlet.

D. Ferron

As it is shown in Fig. 1 the gain of the exchange energy for a weak p - d coupling decreases with an increase of the polaron size. For big J'_{pd} , however, some new effects occur. As it is shown in Fig. 2, for a weak polaron localized on two local spins with half of the carrier density assumed to be localized on each of the local spins, E_{ex} is smaller by a factor ~ 80 than in the case of a small AFP. This effect is a consequence of polaron localization on two local spins which are antiferromagnetically correlated. With an increase of J'_{pd} , instead of the expected saturation a faster increase of E_{ex} for polaron localized on two spins occurs.

An even more pronounced effect is seen for a homogeneously distributed carrier density. As it is shown by squares in Fig. 2, E_{ex} for a weak p - d coupling is practically zero, but sharply increases for J'_{pd} bigger than its critical value. Moreover, a further increase of J'_{pd} is accompanied with a step-like increase of E_{ex} . Studies of the spin structure shows that this critical behavior is caused by a breakdown of the AF bonds and the formation of a magnetic moment in the antiferromagnetic medium S_i . Such a magnetic polaron is known as ferron and it has been described by Kasuya and Yanaka and independently by Nagaev^{24,27}. In the whole range of J'_{pd} values there is no considerable difference between the 1D and 2D AF, similarly to the case of the small AFP.

The spin structure of a ferron localized on two local spins is complex. The correlator of the carrier spin s with the two local AF spins S_p , $\langle sS_p \rangle$, is negative (for antiferromagnetic p - d coupling) for the whole range of J'_{pd} . For a weak J'_{pd} the correlator $\langle sS_p \rangle$ increases lin-

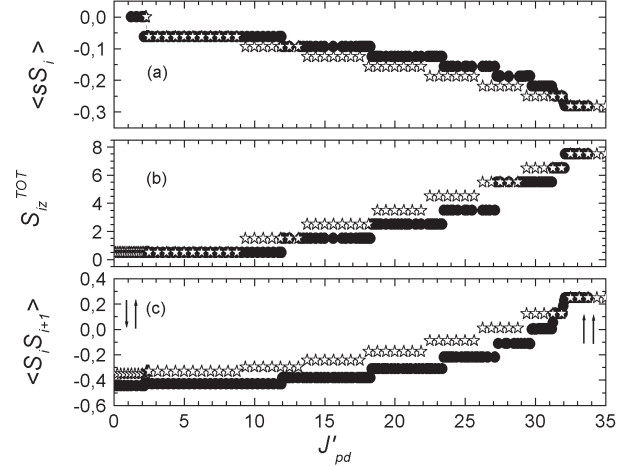


FIG. 4: The correlator between the carrier spin and one of AF spin $\langle sS_i \rangle$ (a), the total spin moment of the AFP polaron, S_{iz}^{tot} , (b), and the correlator between two nearest AF spins $\langle S_iS_{i+1} \rangle$ (c) as a function of J'_{pd} for a homogeneously distributed trial function. The case of a 1D chain of 16 spins with PBC is presented by circles, the 2D 4×4 square with PBC is shown by open stars.

early, then saturates for very large J'_{pd} approaching the limit value of -0.5 . The sharper increase of the energy gain which is seen for $J'_{pd} \cong 2.5$ is caused by a spin-flip of the two local spins, S_p . The systematic increase of E_{ex} , faster than the linear increase, for $J'_{pd} > 4$ originates neither from the correlation $\langle sS_p \rangle$ nor from the correlation between two local spins $\langle S_{p1}S_{p2} \rangle$ but results from a systematic reconstruction of the AF environment of the ferron. The correlation of each of the S_p with surrounding spins, S_i , gradually decreases. Simultaneously, there appears a reconstruction of d - d couplings among the surrounding spins.

More apparent data about the mechanisms of the formation of a ferron can be found if one assumes a homogeneous distribution of the carrier on the AF cluster with periodic boundary conditions. The data are shown in Fig. 4. The correlator between one of the AF spins and the carrier spin as a function of J'_{pd} is presented in Fig. 4a. The step-like behavior of $\langle sS_i \rangle$ is visible for 1D as for 2D case. For $J'_{pd} < 2.5$ correlator $\langle sS_i \rangle$ as well as the gain of the exchange energy is equal zero. For $J'_{pd} > 2.5$ E_{ex} increases in accordance with the observed steps of $\langle sS_i \rangle$. In Fig. 4b the total magnetic moment of the polaron, $S_{iz}^{tot} = \sum_i S_{iz} + s_z$ is presented. It is also characterized by steps occurring for the same values of J'_{pd} as those of $\langle sS_i \rangle$, when J'_{pd} is large. For small $J'_{pd} < 9$ and 2D case the total magnetic moment is equal to $1/2$. For $J'_{pd} < 2.5$ this moment is located at the carrier, for $J'_{pd} > 2.5$ it is a result of the cou-

pling of the electron spin ($s_z = 1/2$) with $\sum_i S_{iz} = 1$ AF spin. The correlator between two neighbor AF spins $|\langle S_i S_{i+1} \rangle|$ is presented in Fig. 4c. It changes from -0.4 for a pure AF to 0.25 (both spins parallel) with an increase in the strength of p - d coupling. At the same time the total magnetic moment, S_{iz}^{tot} , approaches value 7.5 (all bonds broken). Here, it is worth noticing that the step-like behavior of $|\langle S_i S_{i+1} \rangle|$ is not a consequence of breaking of the subsequent bonds but it is associated with steps of the total magnetic moment of the system.

Summarizing, the feron can form when homogeneous, Curie-Weiss magnetization is induced. Our results complete well the classical model of feron.

E. Comb-Like AFP

A homogeneous distribution of the carrier on many AF spins makes the gain of exchange energy on opposite spins cancel each other. Thus we choose a carrier trial function which is distributed on one of the Neel sublattices, which should be intuitively energetically favorable. The carrier distribution is described as follows:

$$|\varphi(i)|^2 = f(r_i) \cos^2\left(\frac{\pi}{2a}r_i\right), \quad (23)$$

where $f(r_i)$ is an envelope function. Usually we assume that it has a Gaussian shape.

Such a polaron we call comb-like AFP^{21,25}.

The gain of the exchange energy versus J'_{pd} for the comb-like polaron with a Gaussian envelope function is presented by triangles in Fig.1. For a small polaron radius the comb-like AFP is equivalent to the small AFP. For a bigger radius the gain is decreasing but it is still much greater than that for large AFP. The exchange energy gain for a large comb-like AFP is only three times smaller than that of a small AFP. This is connected with the decrease of quantum fluctuations (see part IIIF).

The comb-like AFP induces a staggered magnetization in the AF medium. This is shown in Fig. 5a, where the mean value of the correlator between the carrier spin s and the spins of the AF sublattice on which the polaron is acting S_A , $|\langle sS_A \rangle|$, and the spins of other sublattice S_B , $\langle sS_B \rangle$, are presented by circles and squares respectively. The values of the correlators increase linearly for small p - d coupling and they saturate when $J'_{pd} > 1$. The saturation value for $\langle sS_B \rangle$ is equal to 0.25 and it is independent of the number of spins. The saturation value of $|\langle sS_A \rangle|$ is bigger than 0.25 and depends on the number of spins. The difference between the magnetization of the A and B sublattices gives the net magnetic moment of AF.

The part of the magnetic moment which is transferred from the carrier to the AF medium depends on J'_{pd} , as

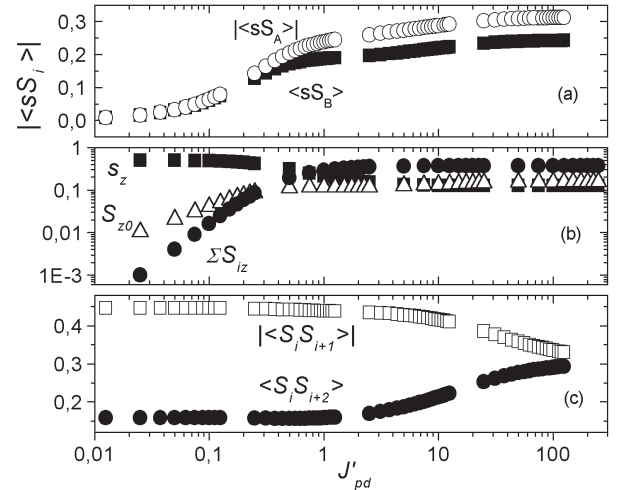


FIG. 5: (a) The mean value of the correlator between the carrier spin s and the spins of the AF sublattice on which the polaron is acting S_A , $|\langle sS_A \rangle|$ (open circles), and the spins of other sublattice S_B , $\langle sS_B \rangle$ (filled squares) as a function of J'_{pd} for a comb-like trial function. (b) The z-component of the carrier spin, s_z (filled squares), the central spin S_{0z} (open triangles), as well as the sum of AF spins $\sum_i S_{iz}$ (filled circles) for an open chain of 16 spins as a function of J'_{pd} . (c) The correlator between the spins from the same sublattice $\langle S_i S_{i+2} \rangle$ (filled circles) and from two neighbor sublattices $|\langle S_i S_{i+1} \rangle|$ (open squares) as a function of J'_{pd} .

it is shown in Fig. 5b. Here the change versus J'_{pd} of z -components of the carrier spin, s_z , of one of the spins on which the carrier acts, S_{0z} , and of the total spin, $\sum_i S_{iz}$, is presented. For small values of p - d coupling a quadratic increase of the moment transferred to AF is observed. $\sum_i S_{iz}$ saturates at a value smaller than 0.5 . Simultaneously, the z -component of the carrier spin decreases from 0.5 for weak p - d coupling to the saturation value of 0.15 for an AF cluster consisting of 16 spins. However, the sum of s_z and $\sum_i S_{iz}$ is constant in whole range of J'_{pd} and equal to 0.5 .

The presence of the comb-like AFP on one of the Neel sublattices breaks the translation symmetry and leads to the formation of two magnetized sublattices. In Fig. 5c the correlators with the nearest neighbor, $|\langle S_i S_{i+1} \rangle|$, and the next nearest neighbor, $\langle S_i S_{i+2} \rangle$, are presented as a function of J'_{pd} . While $|\langle S_i S_{i+1} \rangle|$ decreases for large J'_{pd} , the correlator with the next nearest neighbor increases. Thus, a comb-like AFP increases the AF correlation radius. In the limit of very large J'_{pd} and not too small sizes of the AF cluster the comb-like AFP transforms the antiferromagnet into a classical one.

Although gain of the exchange energy for the comb-like AFP is large the probability of its formation is

small, because it is characterized by a big kinetic energy. Moreover, the comb-like AFP has a tendency to localize into small AFP. This comes from the fact that the kinetic energy is almost the same for both types of polarons (as long as only hopping to the nearest neighbor is taken into account) while the gain of exchange energy due to quantum fluctuations increases three times with localization.

F. Quantum Effect

In this section we summarize the results concerning the formation mechanisms of different magnetic polarons. We pay particular attention to the appearance of quantum effects and we discuss the universality of the Millis, Monien and Pines¹⁰ phenomenological susceptibility approach.

In paragraphs A-E five types of antiferromagnetic polarons were presented. The formation of weak small and medium polarons as well as comb-like polarons is associated with the induction of staggered magnetization. In contrast, the formation of a strong Zhang-Rice polaron is caused by the compensation of the AF spin by the carrier spin. The mechanism of ferron formation is the breaking of AF bonds which is equivalent to the induction of a homogenous magnetic moment.

Classically, the only possible mechanism of AF polaron formation at zero temperature is the turning of the spins in the direction of the effective field induced by the carrier spin. This is the mechanism of ferron formation described by Kasuya and Yanaka²⁴. However, this mechanism does not explain the formation of the remaining polarons. The induction of staggered magnetization is directly associated with the quantum treatment of the antiferromagnet. In a quantum antiferromagnet the ground state is a combination of Neel states, hence no sublattice is distinguished. The simplest measure of AF quantum fluctuations is the difference between the ground and first excited states which are both composed of Neel states. In the presence of staggered magnetization the Neel sublattices start to be distinguishable and the damping of spin fluctuations occurs (see Wilamowski et al.²⁸)

The mechanism of compensation responsible for the formation of the Zhang-Rice polaron should be also considered in a quantum approach. Classically, the carrier couples to the AF spin and such coupling does not destroy the order of the antiferromagnetic cluster. As we have shown in Fig. 3c, in the quantum treatment of the antiferromagnet the affected AF spin may cease to be correlated with neighbor spins. It means that only the quantum approach allows to model the destruction of antiferromagnetic order which is observed

in experiments²⁹.

Despite the quantum character of the discussed above mechanisms there are some particular situations where the polarons can be described in the classical limit, but the quantum corrections have to be taken into account. These corrections are the result of scaling of spin fluctuations with the number of spins and seem to be important for the antiferromagnetic sign of coupling between the AF spin and the spin of the carrier.

By a careful analysis of the dependence of E_{ex} on p - d coupling in the range of very large J'_{pd} we have found that $E_{ex} = \sum_i j_{pd}(i) \langle sS_i \rangle$, where the summation is taken over the N spins S_i within the polaron size (see Fig. 2). The correlator depends on N and is equal to

$$\langle sS_i \rangle = (0.25 + 1/2N). \quad (24)$$

Thus the gain of exchange energy changes from $0.75J'_{pd}$ for a polaron localized on one spin to $0.25J'_{pd}$ for a polaron interacting with an infinite number of spins. It is, hence, possible to calculate the energy of strong small polarons as well as ferrons classically, but the appropriate scalar spin multiplication (0.25) has to be replaced by the quantum factor given by Eq. 24. It is worth noticing that in the limit when N tends to infinity the quantum factor approaches the classical value, whereas for $N = 1$ it is three times bigger.

The same quantum factor 3 is lost when the Zhang-Rice polaron is delocalized on one of the Neel sublattices forming the comb-like polaron.

The importance of the sign of the p - d coupling is shown in the inset to Fig. 2. Here the gain of the exchange energy for a small AFP with a positive and negative sign of p - d coupling is presented. Different slopes of the energy gain for ferromagnetic and antiferromagnetic coupling are observed. It is a consequence of the fact that the carrier spin and AF spins can not couple ferromagnetically to more than 0.25 while for antiferromagnetic coupling the value of correlator $\langle sS_i \rangle$ approaches -0.75 . Thus, only for antiferromagnetic coupling the corrections associated with the number of spins in the AF system are important. In the case of ferromagnetic coupling the classical energy calculations for small polarons and ferrons are correct.

The formula for the exchange energy gain derived on the basis of Pines's phenomenological susceptibility approach gives quite a good qualitative description of the numerical results. However, a detailed comparison of the analytical and numerical results shows that the phenomenological parameter χ_{q_0} scales differently with the AF correlation range ξ for various types of polarons. The response of the AF medium depends on the kind

of magnetic polaron. While $\chi_{q0} \propto \xi$ in 1D it is proportional to ξ^2 in 2D for a small AFP. Moreover χ_{q0} scales differently for large and small polarons in the same dimension. Thus, because of the presence of quantum effects, the phenomenological parameter χ_{q0} can not be treated as universal one.

We conclude that for the description of AFP the classical approach is not sufficient and strictly quantum calculations should be performed.

IV. PHASE DIAGRAM OF MAGNETIC POLARONS

Until now we have considered the gain of exchange energy from magnetic polarons formation and we described the spin structure of various polarons. However the total energy (exchange, phonon and kinetic one) should be taken into account to specify which type of polaron forms. In this section we consider the formation of a pure magnetic polaron. In the next chapter we compare the phonon and magnetic contributions to the formation of polarons in high- T_c superconductors.

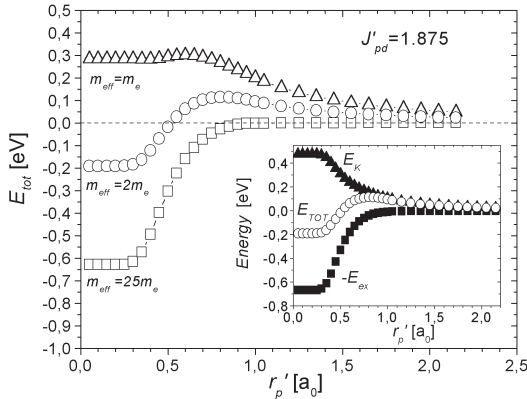


FIG. 6: Total energy, E_{tot} , as a function of polaron radius r'_p for $J'_pd = 1.875$ and effective masses of m_e (triangles), $2m_e$ (circles), $25m_e$ (squares). In the inset the kinetic, exchange, and total energies for the $m_{eff} = 2m_e$ are shown as a function of polaron radius for $J'_pd = 1.875$.

The inset to Fig. 6 presents the dependence of exchange and kinetic energies as well as their sum on the polaron radius for a 2D square cluster with PBC, for $m_{eff} = 2m_e$ and $J'_pd = 1.875$. The exchange energy behaves as in Fig. 1. The kinetic energy is equal to $4t_1$ for polaron localized in one elementary cell and it decreases like as $1/r_p'^2$ for a larger polaron radius in accord with Eq. 6. The total energy has a flat minimum in the range of $0 < r'_p < 0.25$ allowing only a small AFP to form. The value of total energy is equal -0.2 eV.

In Fig. 6 the total energy as a function of polaron radius calculated for a few chosen effective masses is shown. It can be seen that for $m_{eff} = m_e$ no AFP can form. For a large m_{eff} (which scales as $1/t_1$) the only polaron which can exist is the small one. The formation of a ferron is not possible because J'_pd is too small. The medium and large polarons tend to localize in one elementary cell, independently of the values of the effective mass and t_1 . The tendency to localization is associated with a rapid reduction of the exchange energy gain with increasing polaron radius, which is directly connected with quantum fluctuations of the AF medium (see part IIIF). We have found that for $J'_pd = 1.875$ magnetic polarons can form only if the effective mass is higher than the critical value of $1.6m_e$ what corresponds to $t_1 = 2J_{dd}$. For weaker $p-d$ couplings the small AFP is also the only polaron which can form but its effective mass should be much greater.

In Fig. 7 the phase diagram of the formation of different magnetic polarons is shown. The area of parameters t_1 and J'_pd for which the small AFP forms is marked by a solid line.

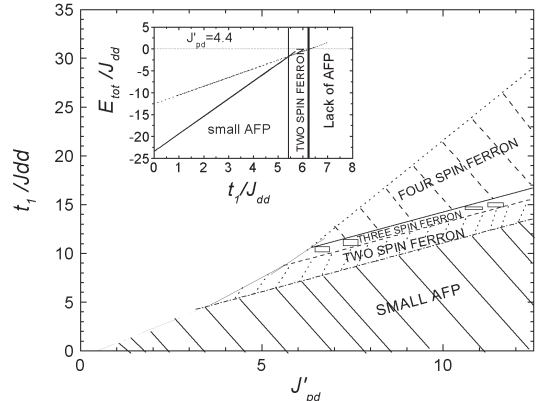


FIG. 7: Phase diagram of magnetic polaron formation (on x axis the ratio of $p-d$ to $d-d$ coupling constants normalized by the number of AF bonds, J'_pd , on y axis t_1 in J_{dd} units). In the inset E_{tot} as a function of t_1 for $J'_pd = 4.4$ is shown.

For higher J'_pd values the small ferrons can also form. In the inset to Fig. 7 the total energies of a small AFP and a small ferron are compared. Here $J'_pd = 4.4$. The gain of the exchange energy of a small AFP is higher than for the two spin ferron and it is constant. The kinetic energy of two-spin ferron (polaron localized on two neighboring spins) is smaller than that of a small AFP (localized in one elementary cell) and scales linearly with t_1 . Thus the total energies of both polarons are linear functions of t_1 but with different slopes. In particular the boundary between small AFP and two spin ferron for $J'_pd = 4.4$ crosses for $t_1 = 5.4J_{dd}$ what

is equivalent to $m_{eff} \geq 0.6m_e$. For t_1 which is greater than $6.25J_{dd}$ any AFP is not formed. In general the small AFP forms for effective masses larger or equivalent to one electron mass, while the two-spin ferron appears for masses smaller than one electron mass.

Proceeding similarly we found the range of parameters for which also other types of polarons can form. In Fig. 7 the ranges where small AFP, two, four-spin ferrons can occur are shaded by solid, dotted and dashed lines respectively. The appearance of a three-spin ferron is indicated by rectangles. Larger ferrons appear for much stronger p - d couplings and we omit their description because they would exist for unphysical parameters.

The presented results were calculated for a 2D square with PBC. However, we have found that the phase diagram is not very dependent on the shape of the 2D AF cluster. For different 2D clusters the formation range of subsequent polarons can be shifted about 10%–15%.

The investigation of polaron formation in a wide range of parameters is exceptionally valuable when we want to classify which type of polaron could be formed in different materials. For example in doped EuTe where J_{pd} is about 0.125 eV and J_{dd} amounts to 0.002 eV³⁰ the p - d coupling on one AF bonds $J'_{pd} \approx 8$. At the same time $t_1 \approx 15J_{dd}$. For such parameters our model predicts the ferrons formation (see Fig. 7) in accord with experiments (see^{24,30} and references therein).

In high- T_c superconductors which are based on CuO₂ layers the d - d exchange coupling is between 0.055 eV and 0.085 eV, as determined from the Neel temperature of antiferromagnetic precursors of superconductors³¹. The value of J_{pd} is determined on the band structure calculations to be about 1–3 eV^{15,32,33,34}. Thus, the ratio of p - d to d - d exchange energies is between 1.5 and 4 under assumption that $J_{dd} = 0.075$ eV. The effective mass is much more difficult to determine because the mass observed in experiments (for example in angle resolved photoemission (ARPES)) is the mass of non-interacting particles, which is decorated by exchange as well as phonon interactions. Since the decorated mass observed in ARPES experiments³⁵ is about $4m_e$ and the mass in our model is dressed only by phonons, the mass which we should consider in the phase diagram is smaller than $4m_e$ which is equivalent to $t_1 > 0.8J_{dd}$.

We conclude, on the basis of our phase diagram, that for parameters typical for weakly doped high- T_c superconductors the small AFP would mainly form. There may be also some competition between the formation of small AFP and two-spin ferrons provided that the effective mass dressed in phonons is a bit lower than the electron mass. Large AFP have energies of few orders of magnitude lower than those of small AFP and ferrons.

We would like to emphasize that formation of small size polarons in weakly doped high- T_c superconductors is associated with the destruction of the AF order²⁸. In this sense the use of small AF clusters in our model is justified.

V. THE CONTRIBUTION OF PHONON AND MAGNETIC POLARON

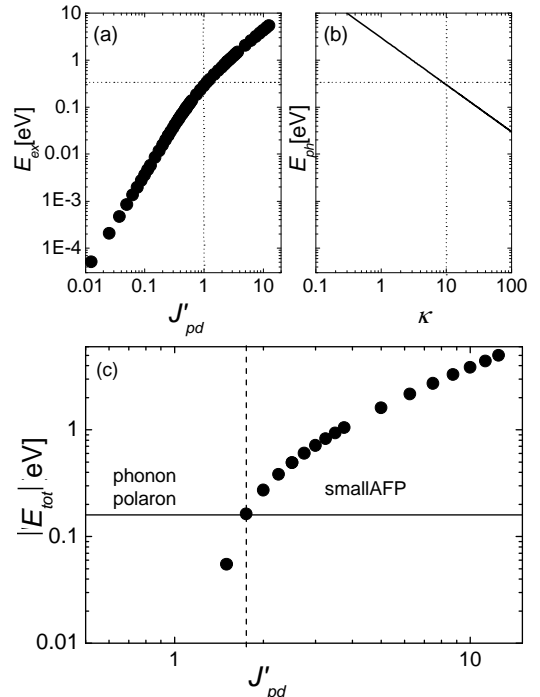


FIG. 8: The gain of exchange energy, E_{ex} from the formation of a small AFP as a function of J'_{pd} (a). The phonon energy, E_{ph} , versus effective dielectric constant κ (b). The absolute value of the total energy for a magnetic polaron (circles) and for a phonon polaron (solid line) as a function of J'_{pd} (c). Here, $m_{eff} = 2.2m_e$ and $\kappa = 5$. The vertical dashed line shows the value of J'_{pd} where the magnetic and phonon polaron energies are equal.

Now we will compare the phonon and magnetic contributions to the formation of polarons in weakly doped high- T_c superconductors. We showed that in the 2D case the gain of exchange energy from the formation of large magnetic polarons is closed to zero and they are unlikely to form (Fig. 6 and Fig. 7). Since Mott and Alexeev⁸ suggest that in high- T_c superconductors only small phonon polarons form (see Eq. (12)). We will not consider here large polarons, neither of magnetic nor phonon origin.

In Fig. 8a the gain of the exchange energy due to the formation of a small magnetic polaron in a 2D AF square cluster with PBC is shown as a function of J'_{pd} . In Fig. 8b the energy gain due to the formation of phonon polaron is presented as a function of κ . κ is defined as the difference between the static, ε_0 , and high frequency, ε , dielectric constants. Typical values of κ are between 5 and 20. The kinetic energy for both small polarons is the same, $E_k = 4|t_1|$, and is omitted for clarity.

Horizontal and vertical dotted lines drawn in Figs. 8a and 8b indicate parameter values for which the energy gain is the same for both phonon and magnetic polarons. We found that the energy gain for both polarons is identical and equal to 0.35 eV for $J'_{pd} = 1$ and $\kappa = 10$. The energy gain due to the formation of phonon polarons is greater than that for magnetic polarons for $\kappa < 10$ and $J'_{pd} < 1$. For $\kappa > 10$ and $J'_{pd} > 1$ the magnetic polaron dominates. One can see that for the range of parameters which seem to be typical for high- T_c superconductors the energy gain due to the formation of phonon and magnetic polarons is comparable and of the order of fraction of electronvolt.

In order to obtain the total energy of magnetic and phonon polaron separately, E_{tot} , we have evaluated the kinetic energy for a chosen set of parameters: $m_{eff} = 2.2m_e$ and $\kappa = 5$, which are reasonable for high- T_c superconductors. In Fig. 8c we show the values of E_{tot} for phonon as well as magnetic polarons versus J'_{pd} . For the phonon polaron E_{tot} is constant and equal to 0.15 eV, since according to Eq. 7 the phonon as well as kinetic energies are independent of J'_{pd} .

The phonon polaron dominates in the range of weak p - d couplings. In contrast the magnetic polaron (circles in Fig. 8c) dominates in the range of strong J'_{pd} where its energy increases linearly with J'_{pd} . In the range of $J'_{pd} = 1.5 - 4$ which is typical for weakly doped high- T_c superconductors the energies of both polarons are comparable or magnetic polaron energy slightly overcomes the energy of phonon one. This result agrees well with

very recent paper³⁶ which stresses the importance of phonon interactions in high- T_c superconductors.

We conclude that within our model the phonon and magnetic polaron energies are comparable and both contributions should be included in the total polaron energy in high- T_c superconductors.

VI. SUMMARY

Using the Spin-Fermion model and treating all spins in quantum approach we found that depending on the material parameters five various types of magnetic polarons in antiferromagnetic medium can be distinguished.

We showed that in the range of parameters typical for weakly doped high- T_c superconductors the contributions of phonon and magnetic interactions to the formation of a polaron are comparable and hybrid magnetic-phonon polarons form.

In weakly doped high- T_c superconductors small magnetic polarons as well as small ferrons form. Our numerical study allows to find a continuous evolution from Zhang-Rice approach, when p - d coupling is assumed to be much stronger than d - d coupling, via important for high- T_c materials intermediate range, to linear response approach suitable for weak p - d coupling.

Comb-like polarons can not form when the band is empty (i.e. in undoped material) because of cost of high kinetic energy. However, they can play a fundamental role in doped high- T_c materials when the band is partially filled^{21,25}.

Acknowledgements

Valuable discussion with H. Przybylińska. Work supported by the KBN grant 2 P03B 007 16.

¹ M. R. Norman, H. Ding, M. Randeria, J. C. Campuzano, T. Yokoya, T. Takahashi, T. Mochiku, K. Kadouwaki, P. Guptasarma, and D. G. Hinks, *Nature* **392**, 157 (2000).

² K. Karpińska, M. Z. Cieplak, S. Guha, A. Malinowski, T. Skośkiewicz, W. Plesiewicz, M. Berkowski, B. Boyce, T. R. Lemberger, and P. Lindenfeld, *Phys. Rev. Lett.* **84**, 155 (2000).

³ B. G. Levi, *Phys. Today* **17**, 53 (2000).

⁴ C. Castellani, C. D. Castro, and M. Grilli, *Phys. Rev. Lett.* **75**, 4650 (1995).

⁵ S. I. Pekar, *Zh. Eksp. Teor. Fiz.* **16**, 335 (1951).

⁶ H. Fröhlich, *Phys. Rev.* **79**, 845 (1954).

⁷ H. Fröhlich, *Adv. Phys.* **3**, 325 (1954).

⁸ A. S. Alexandrov and N. Mott, *Polarons and Bipolarons* (World Scientific, Singapore, 1995).

⁹ A. S. Alexandrov, *Phys. Rev. B* **38**, 925 (1988).

¹⁰ A. Millis, H. Monien, and D. Pines, *Phys. Rev. B* **43**, 258 (1991).

¹¹ F. C. Zhang and T. M. Rice, *Phys. Rev. B* **37**, 3759 (1988).

¹² E. Dagotto, *Rev. Mod. Phys.* **66**, 763 (1994).

¹³ S. R. White and D. J. Scalapino, Phys. Rev. Lett. **84**, 3021 (2000).

¹⁴ C. Hellberg and E. Manousakis, Phys. Rev. Lett. **84**, 3022 (2000).

¹⁵ C. Buhler, S. Yunoki, and A. Moreo, Phys. Rev. Lett. **84**, 2690 (2000).

¹⁶ J. Riera and E. Dagotto, Phys. Rev. B **57**, 8609 (1998).

¹⁷ J. Zaanen, Nature **404**, 714 (2000).

¹⁸ H. A. Mook, P. Dai, F. Dogan, and R. Hunt, Nature **404**, 729 (2000).

¹⁹ R. P. Sharma, S. B. Ogale, Z. H. Zhang, J. R. Liu, W. K. Chu, B. Veal, A. Paulikas, H. Zheng, and T. Venkatesan, Nature **404**, 736 (2000).

²⁰ B. L. Altshuler, L. B. Ioffe, and A. J. Millis, Phys. Rev. B **52**, 5563 (1995).

²¹ E. M. Hankiewicz, R. Buczko, and Z. Wilamowski, Physica B **284-288**, 437 (2000).

²² J. R. Schrieffer, J. Low Temp. Phys. **99**, 397 (1995).

²³ M. Hamada and H. Shimahara, Phys. Rev. B **51**, 3027 (1995).

²⁴ T. Kasuya and A. Yanase, Rev. Mod. Phys. **40**, 684 (1968).

²⁵ E. M. Hankiewicz, R. Buczko, and Z. Wilamowski, Acta Phys. Polonica A **97**, 185 (2000).

²⁶ M. Laukamp, G. B. Martins, C. Gazza, A. L. Malvezzi, E. Dagotto, P. M. Hansenand, A. C. López, and J. Riera, Phys. Rev. B **57**, 10755 (1998).

²⁷ V. D. Lakhno and E. Nagaev, Fiz. Tverdogo Tela **18**, 3429 (1976).

²⁸ Z. Wilamowski and E. M. Hankiewicz, Acta Phys. Polonica A **97**, 403 (2000).

²⁹ R. J. Birgeneau, D. R. Gabbe, H. P. Jenssen, M. A. Kastner, P. J. Picone, T. R. Thurston, G. Shiraneand, Y. Endoh, M. Sato, K. Yamada, et al., Phys. Rev. B **38**, 6614 (1988).

³⁰ P. Wachter, in *Handbook on the Physics and Chemistry of the Rare Earths* (1979), p. 507, eds. K.A. Geschneider, Jr. and L. Eyring.

³¹ N. M. Plakida, *High Temperature Superconductivity* (Springer Verlag, Berlin, 1995).

³² M. S. Hybertsen, E. B. Stechel, M. Schluter, and D. J. Jinnison, Phys. Rev. B **41**, 11068 (1990).

³³ H. Eskes, L. H. Tjeng, and G. Sawatzky, Phys. Rev. B **41**, 288 (1990).

³⁴ C. X. Chen, H. B. Schüttler, and A. J. Fredro, Phys. Rev. B **41**, 2581 (1990).

³⁵ G. Mante, R. Claessen, T. Buslaps, S. Harmand, R. Manzke, M. Skibowski, and J. Fink, Z. Phys. B **80**, 181 (1990).

³⁶ A. Lanza, P. V. Bogdanov, X. J. Zhou, S. A. Kellar, D. L. Feng, E. D. Lu, T. Yoshida, H. Eisaki, A. Fujimori, K. Kishio, et al., Nature **412**, 510 (2001).